Front. Earth Sci. 2023, 17(3): 788–796
https://doi.org/10.1007/s11707-022-1059-1

RESEARCH ARTICLE

Comparative experimental study on porosity, mechanical and CO_2 adsorption characteristics of coal and shale

Haitao LI[1], Guo YU[2], Xiaolei WANG (✉)[3], Dongming ZHANG[3,4]

1 Exploration and Development Research Institute of PetroChina, Southwest Oil and Gas Field Company, Chengdu 610051, China
2 PetroChina Southwest Oil and Gas Field Company Planning Department, Chengdu 610051, China
3 State Key Laboratory of Coal Mine Disaster Dynamics and Control, Chongqing University, Chongqing 400044, China
4 School of Resources and Environmental Engineering, Jiangxi University of Science and Technology, Ganzhou 341000, China

Abstract To compare the pore structure, mechanical and CO_2 adsorption properties of coal and shale, a series of experiments were carried out using nuclear magnetic resonance (NMR), uniaxial compression, Brazilian splitting, and high-pressure CO_2 adsorption. The results show that the total porosity of coal is 7.51 times that of shale, and shale is dominated by adsorption pores, while adsorption pores and seepage pores in coal are equally important. Moreover, it is found that the micropores in shale are more advantageous, while meso-macropore in coal are more significant. The adsorption pore surface of coal is rougher than that of shale, and the seepage pore structure of shale is more complex. The uniaxial compressive strength, elastic modulus and absorption energy of shale are 2.01 times, 2.85 times, and 1.27 times that of coal, respectively, indicating that shale has higher compressive capacity and resistance to elastic deformation than coal. The average tensile strength, Brazilian splitting modulus, absorbed energy and brittleness index of shale are 7.92 times, 6.68 times, 10.78 times, and 4.37 times that of coal, respectively, indicating that shale has higher tensile strength and brittleness, but lower ductility, compared with coal. The performed analyses show that under the same conditions, the CO_2 adsorption capacity of coal is greater than that of shale. The present article can provide a theoretical basis to implement CO_2-enhanced coalbed methane (CBM)/shale gas extraction.

Keywords coal, shale, NMR, mechanical properties, adsorption characteristic

1 Introduction

Coalbed methane and shale gas, as two forms of unconventional natural gas, which can provide a clean and efficient energy supply (Wang et al., 2018b; Liu et al., 2022b; Wang et al., 2022b). Recently, remarkable achievements have been made regarding this abundant source of energy. In the southern Qinshui Basin, China, the development of coalbed methane has entered the stage of commercial exploitation, and at the same time, exploitation of the shale gas in the Sichuan Basin has reached its historical peak (Chen et al., 2010; Wang et al., 2011). Coal and shale are similar porous media that can store methane in their porous structures (Wang et al., 2018a; Wang et al., 2021a; Liu et al., 2022c; Yang et al., 2022a). Therefore, it is necessary to investigate the differences between their pore structure to deeply understand the gas occurrence characteristics. With the development of technical measures such as hydraulic fracturing in coalbed methane and shale gas extraction, the mechanical properties of coal and shale can be studied to optimize extraction techniques. Moreover, the study of the adsorption capacity of coal and shale for CO_2 can provide a theoretical basis to implement CO_2-enhanced CBM/shale gas extraction.

A review of the literature indicates that the characterization techniques for the pore structure of porous media are relatively mature. In this regard, numerous methods, including irradiation methods (e.g. scanning electron microscopy (SEM), micro-computer tomography (CT), and nuclear magnetic resonance (NMR)), and fluid intrusion methods (e.g. mercury intrusion methods and low-pressure N_2/CO_2 adsorption methods) have been proposed (Gao et al., 2022; Wang et al., 2022a; Wang et al., 2020; Zheng et al., 2022). Cao et al. (2015) adopted the low-pressure N_2 adsorption method and mercury intrusion method and used a scanning electron microscope to analyze the difference between the pore structure of coal and shale. The results showed that the pores of coal are mainly smaller than 17.11 nm, while the

Received October 7, 2022; accepted November 29, 2022

E-mail: wxl_pessimist@cqu.edu.cn

pores of shale are mainly micro-scale. Wu et al. (2020) compared the pore structures of coal and shale by analyzing the adsorption of low-pressure N_2 and CO_2 gases and using the mercury intrusion method. It was found that mesopores of shale are more developed, while the micropores of coal are more developed. Based on low-pressure adsorption of N_2, Zhang et al. (2017) analyzed the pore differences between high-rank coal and shale in the Shanxi Formation and found that micro-scale pores are dominant in shale, while small pores are dominant in coal. Although remarkable results were achieved in the reviewed investigations, the pore characterization method is applicable only to test granular samples, and the intrusion of high-pressure mercury destroys the original pore structure of samples. Comparatively, the NMR test causes less damage, has faster detection, and can test larger samples (Wang et al., 2019). Accordingly, NMR can be applied to conduct more comprehensive tests on the pores of coal and shale. Among different methods for determining the pore structure of cylindrical coal samples, CT is limited by its resolution, so it is more suitable to analyze micron-scale pores. Meanwhile, variations of the coal pore are typically very small before and after CO_2 adsorption, while CT technology relies on threshold segmentation in image post-processing so the occurrence of large errors is undeniable. Therefore, the NMR method is applied in the present study to characterize the pore structure of coal and shale.

The mechanical properties of coal and shale are significantly different. Although numerous investigations have been carried out on the mechanical properties of coal and shale, there is no comparative report. Wang et al. (2022c) analyzed the mechanical properties of coal with different bedding angles by Brazil splitting test and showed that the peak loading force of coal is concentrated at 2.06−3.01 kN. Moreover, Zhang et al. (2019) performed uniaxial compression experiments and tested the mechanical properties of coal. It was found that the uniaxial compression strength (UCS) and elastic modulus of coal are 46.07 MPa and 3.37 GPa, respectively. Yang et al. (2022b) carried out experiments and showed that UCS and elastic modulus of shale are 256.1 MPa and 25.27 GPa, respectively. Considering the significance of coal and shale in unconventional gas extraction, the difference between the mechanical properties of coal and shale should be further investigated.

Studies show that coal and shale have different pore structures, so they have significantly different gas adsorption capacities (Wang et al., 2021c). In this regard, Wang et al. (2021b) analyzed the CO_2 adsorption in primary and structural coal and found that since the pores of structural coal are more developed than primary coal, they have a greater CO_2 adsorption capacity that may reach 70 mL/g. Zhou et al. (2018) analyzed the CO_2 adsorption capacity of shale with different maturity levels and concluded that the adsorption capacity of shale for CO_2 varies in the range of 6−8 mL/g.

In the present study, it is intended to study the difference between the pore structures of coal and shale using NMR. Then, uniaxial compression tests and Brazilian splitting experiments are carried out to compare the mechanical properties of coal and shale. Meanwhile, CO_2 adsorption experiments are performed to analyze the difference in adsorption capacities of coal and shale. The results of this study provide a theoretical basis to improve the occurrence mechanism of coalbed methane and shale gas, and a guideline to improve mining technology.

2 Experimental work

2.1 Sampling

The shale samples were collected from the Qiongzhusi Formation on the west bank of Dianchi Lake, south-west of Kunming City, Yunnan Province, and the coal samples were selected from the Yuwang Coal Mine in Yunnan Province. The collected bulk samples were sent to the Chongqing University Coal Mine Hazard Dynamics and Control Laboratory, where samples were cut into 100 mm height and 50 mm diameter cylinders for NMR and uniaxial compression tests. Moreover, 25 mm height and 50 mm diameter discs were prepared for Brazilian splitting tests. The prepared samples are shown in Fig. 1. The chemical compositions of shale and coal samples determined by an X-ray diffractometer are listed in Table 1. It is observed that quartz is the dominant component in shale and coal, followed by illite in shale and calcite in coal.

2.2 Experimental methods

2.2.1 NMR

NMR is an effective method to determine the pore size with little damage to the pores over a wide range covering pores from 0.1 nm to 100000 nm. In the present study, the NMR testing system (Suzhou Newmark Analytical

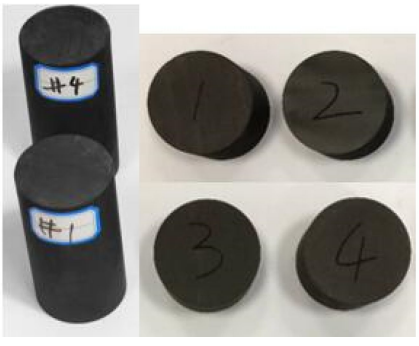

Fig. 1 Experimental sample.

Table 1 Mineral composition of shale and coal (%)

Sample	Quartz	Calcite	Pyrite	Kaolinite	Illite	Chlorite	Dolomite
Coal	41.3	37.2	7.1	5.9	–	–	–
Shale	38.3	7.8	2.6	–	29.9	8.4	7.5

Instrument Co., Ltd. MacroMR12-150H-I, China) and a pulse sequence test (Using Carr-Purcell-Meiboom-Gill) are used in the experiments. The attenuation signal of spin echo string, which reflects the pore size, and the distribution curve of transverse relaxation time (T_2), can be obtained on samples with saturated water and curve fitting. The relationship between T_2 and aperture r can be expressed as follows (Song et al., 2020; Su et al., 2020):

$$\frac{1}{T_2} = \rho \times \frac{S}{V} = F_s(\frac{\rho}{r}), \tag{1}$$

where T_2 is the transverse relaxation time, ms; ρ is the transverse surface relaxation strength, μm/ms; S is pore surface area, cm^2; V is the pore volume, cm^3; F_s is the shape factor of pores; r is the pore radius, m.

The surface irregularity of porous media is measured using the Fractal dimension method, which can characterize the surface complexity and surface roughness of pores in coal and shale. The performed analyses proved that the pore network of coal and shale has fractal characteristics (Chandra et al., 2020; Yang et al., 2020; Geng et al., 2022). Therefore, the NMR method and fractal theory are combined to achieve an effective way to describe the pore structure of coal and shale. In this regard, Chen et al. (2019) established the following spectrum fractal dimension equation through NMR:

$$\lg(w) = (3 - D_N)\lg(T_2) + (D_N - 3)\lg(T_{2\max}), \tag{2}$$

where w is the cumulative porosity percentage when transverse relaxation time is less than T_2; D_N is the fractal dimension; $T_{2\max}$ is the maximum transverse relaxation time, ms.

According to Eq. (2), the slope of the straight line obtained by linear fitting the scatter plot drawn from the relationship between lg(w)–lg(T_2) can be used to calculate the fractal dimension D_N of coal and shale.

2.2.2 Uniaxial compression test

A hydraulic servo mechanical system (MTS 815, MTS, USA) with a maximum axial load of 2800 kN is used to control force, displacement, axial strain, and transverse strain. During the experiments, the displacement control loading mode with a loading rate of 0.1 mm/min was adopted in the uniaxial tests. The elastic modulus (E) of coal and shale was calculated using the elastic segment of the full stress-strain curve of the sample.

The deformation and destruction of coal and shale are accompanied by energy absorption, accumulation, and dissipation. The absorbed energy (U) of the rock failure process was used to investigate the mechanical behavior of the rock. This parameter can be calculated by the area between the curve and the abscissa in the force-displacement curve through the following expression:

$$U = \int_0^{l_i} P_i \mathrm{d}l, \tag{3}$$

where U is absorbed energy, mJ; l_i is displacement of step i, mm; P_i is load of step i, N.

2.2.3 Brazil splitting test

An IS material testing machine (AG-250kN, Shimadzu Company, Japan) with a maximum axial load of 250 kN, displacement measurement accuracy of ±0.1%, and a loading rate range of 0.0005–1000 mm/s was used to perform the Brazilian splitting test. Load control and displacement control loading methods can be adopted in the test. In this article, the Brazilian split tests were carried out by displacement-controlled loading, and the loading rate was set to 0.1 mm/min. Considering bedding characteristics of coal samples, 7 bedding angles (0°, 15°, 30°, 45°, 60°, 75°, and 90°) were considered and the tests were labeled 1# to 7#, respectively. The shale studied in this paper had no obvious bedding characteristics, so seven shale samples (Nos. 1#–7#) were considered.

Brazilian splitting tests reflect the tensile failure characteristics of the samples through the following expression (Feng et al., 2019; Liu et al., 2022a):

$$\sigma_t = \frac{2P_{\max}}{\pi D h}, \tag{4}$$

where σ_t is tensile strength, MPa; $P_{\max}$ is peak load, N; D is diameter of sample, mm; h is thickness of sample, mm.

In this test, the Brazilian splitting modulus (E_B) reflects the resistance of samples to elastic deformation, which is helpful to understand the splitting failure characteristics of samples. Yu and Wang (2004) divided the ordinate in the force-displacement curve by the area of the sample meridian plane and the abscissa divided by the sample diameter. In the mapped curve, the slope of the new curve is E_B. The Brazilian fracture absorption energy (U_B) is the same as that of the uniaxial compression test.

The brittleness of samples is a key parameter to evaluate geomechanics. In this regard, Hou et al. (2022) showed that the rock brittleness index (BI) can be calculated by the peak characteristic of the force-displacement curve in the form below:

$$BI = \frac{\sigma_t}{\varepsilon_t}, \tag{5}$$

where BI is brittleness index; ε_t is axial strain at $P_{\max}$ point of peak load.

2.2.4 CO_2 adsorption experiment

According to MT/T 752-1997 standard and the static volume theory (Sing, 1982), HCA high-pressure volume equipment (Chongqing Research Institute of CCTEG, China) was used to conduct high-pressure CO_2 adsorption experiments (Fig. 2). To this end, 50 g of the coal/shale sample (six different particle size ranges: < 0.074, 0.074−0.2, 0.2−0.25, 0.25−0.5, 0.5−1, and 1−3 mm) was placed in a sample container immersed in a 60°C water bath and evacuated. Then the dead space volume of the container was measured using the method proposed by Jin et al. (2016). Finally, the adsorption volume and methane adsorption isotherm were obtained when the methane pressure reached 5 MPa.

The adsorption isotherm data of coal and shale can be fitted by the Lagmuir model, which is widely used in coal and shale fields (Langmuir, 1917; Joubert et al., 1973; Satya et al., 2006):

$$V = \frac{abp}{1+bp}, \tag{6}$$

where V is the volume of adsorbed gas, mL/g; a is the Langmuir constant, mL/g; b is the Langmuir constant, MPa^{-1}; p is the equilibrium pressure, MPa.

3 Results

3.1 Pore structure difference

Based on the obtained results from NMR tests, the nuclear magnetic T_2 spectrum of coal and shale is presented in Fig. 3. It is observed that there are three peaks in the coal and shale spectra. The three peaks of coal are significantly larger than those of shale. Coal samples have the characteristics of "high at both ends, low in the middle", while the peak of shale at 0.1−2 ms is much larger than the other two peaks, and three peaks are decreasing. By analysis of the cumulative porosity test results, the total porosity of coal is 18.199%, while that of shale is only 2.423%. Accordingly, the total porosity of coal is 7.51 times that of shale.

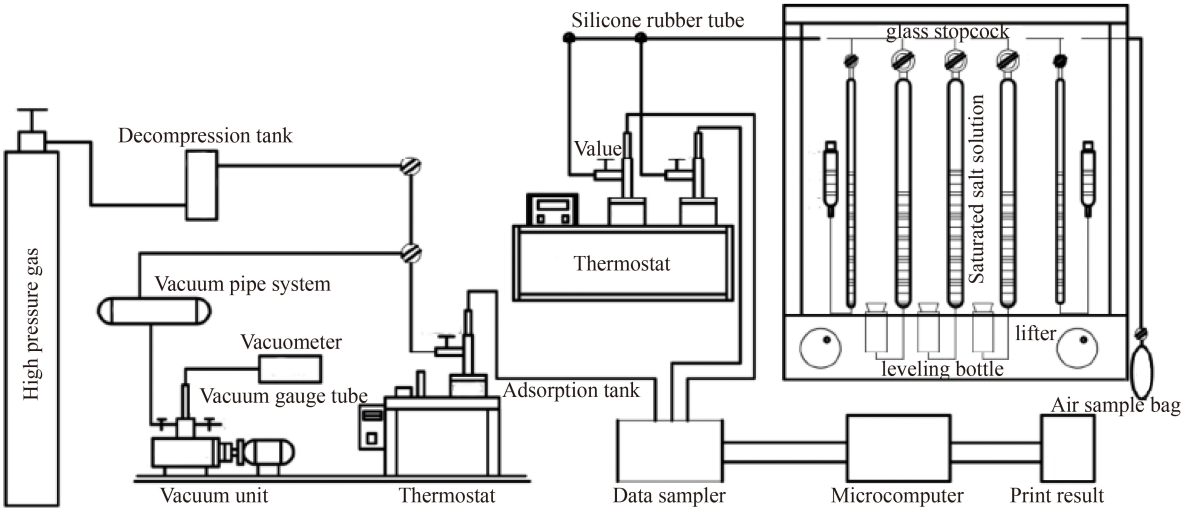

Fig. 2 Equipment of high-pressure gas adsorption with volumetric method.

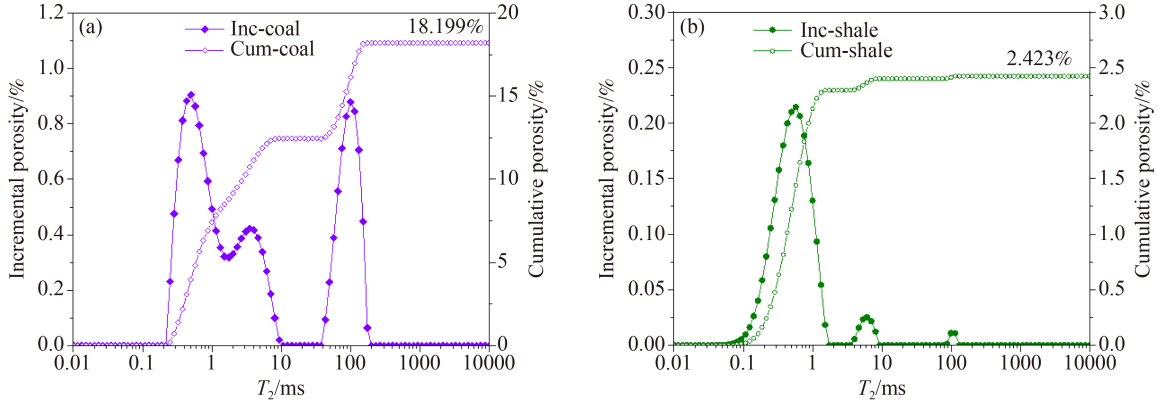

Fig. 3 Nuclear magnetic T_2 spectrum of coal and shale.

Hodot proposed the pore structure classification of micropores (0–10 nm), minipores (10–100 nm), mesopores (100–1000 nm), and macropores (> 1000 nm), in which micropores and minipores are called adsorption pores, and mesopores and macropores are called seepage pores. According to the NMR experiment, the pore size distributions of coal and shale are presented in Fig. 4. It is observed that the proportion of adsorption pores in shale is much larger than that of seepage pores, while the gap between adsorption pores and seepage pores in coal is small. In both adsorption pores, the proportion of adsorption pores of shale is larger than that of coal, while the proportion of seepage pores of shale is smaller than that of coal. Consequently, shale samples mainly contain adsorption pores, while adsorption pores and seepage pores are equally important in coal.

To further analyze the difference between coal and shale in porosity, the proportion of micropores, minipores, mesopores, and macropores are presented in Fig. 5. It is observed that the proportion of micropores, minipores, mesopores, and macropores in shale is 50.58%, 45.06%, 3.41%, and 0.95% respectively, while that in coal is 21.85%, 41.54%, 6.79%, and 29.82%, respectively. It is inferred that micropores and minipores in shale are dominant, while the four pores in coal are equally important. Moreover, it is found that the proportion of micropores and minipores in shale is 2.31 times and 1.08 times that of coal, respectively, indicating that micropores in shale are more advantageous than in coal. The proportion of minipores in shale and coal is almost the same. In addition, the proportion of mesopore and macropore in coal is 1.99 times and 31.39 times that of shale respectively, indicating that the proportion of mesopore and macropore in coal is more significant than that of shale. This is especially more pronounced in macropores.

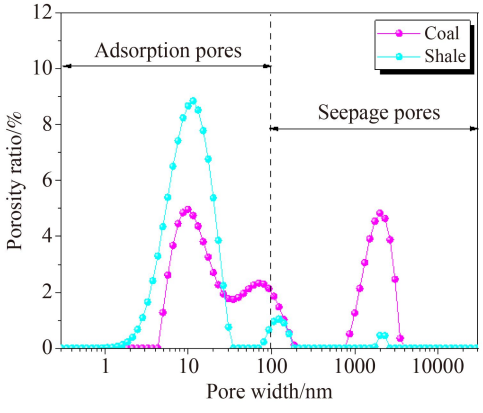

Fig. 4 Nuclear magnetic pore size distribution of coal and shale.

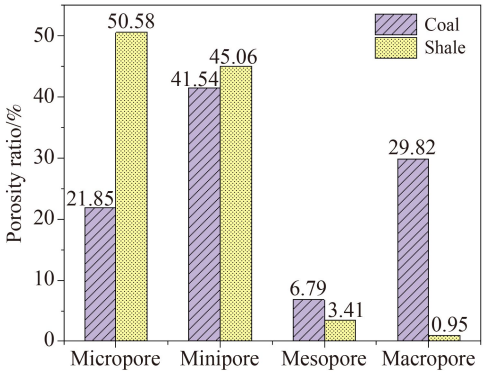

Fig. 5 Porosity ratio of coal and shale.

To compare the pore structure between coal and shale in more detail, the fractal dimension of the two is calculated using Eq. (2), and the results are shown in Fig. 6. According to the division of adsorption pore and seepage pore, $\lg(w)$–$\lg(T_2)$ curve is divided into two parts to obtain the surface fractal dimension D_{N1} of coal and shale adsorption pore and the volume fractal dimension D_{N2} of seepage pore. Generally, the larger the D_{N1}, the higher the pore surface roughness; moreover, the larger the D_{N2}, the more complex the seepage hole structure (Song et al., 2020). According to the fractal dimension results of coal and shale in Fig. 5, the curves can be fitted to a linear line, indicating that the fractal dimension can be used to characterize the pore structure. According to the calculation results of the fractal

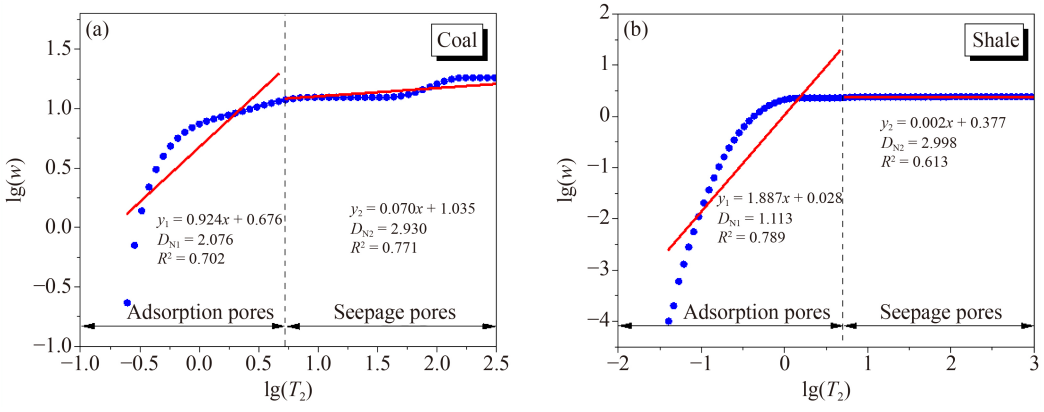

Fig. 6 Fractal dimension of coal and shale.

dimension, D_{N1} of coal and shale is 2.076 and 1.113, respectively, indicating that the surface roughness of the coal adsorption pore is lower than that of shale. Furthermore, D_{N2} of coal and shale is 2.930 and 2.998, respectively, indicating that the seepage pore structure of shale is more complex, but the difference between the two is not obvious. The fractal dimensions of coal and shale show that D_{N2} is greater than D_{N1}, indicating that seepage holes are more complex than adsorption pores (Shao et al., 2017).

3.2 Uniaxial compression characteristic difference

Uniaxial compression tests can well show the difference in mechanical properties of coal and shale samples. The stress-strain curves of coal and shale samples are presented in Fig. 7. The mechanical parameters of coal and shale such as UCS, *E*, and *U* are listed in Table 2.

The results show that both coal and shale samples have similar characteristics with rock stress-strain curves, namely the pore compaction stage, elastic deformation stage, stable development stage of microcracks, and rapid crack growth stage. In the first stage, the pores in coal and shale are gradually compressed, resulting in nonlinear deformation. In this stage, shale and coal have similar stress-strain curves that end at about 0.3%. In the elastic deformation stage, however, the stress-strain curve of shale is linear and the duration is long, while the elastic stage of coal is short. In the third and fourth stages, internal microcracks significantly develop in coal and obvious plastic deformations occur, while these two stages of shale are very short and the fracture is brittle.

The comparison of mechanical parameters in coal and shale shows that the UCS of shale is 2.01 times that of coal, indicating that shale has a stronger compressive capacity than coal. Moreover, the *E* of shale is 2.85 times that of coal, indicating that shale has more resistance to elastic deformation. The absorption energy of shale before fracture is 1.27 times that of coal, indicating that higher levels of energy are required to destruct shale samples, demonstrating that shale has a higher resistance to destruction.

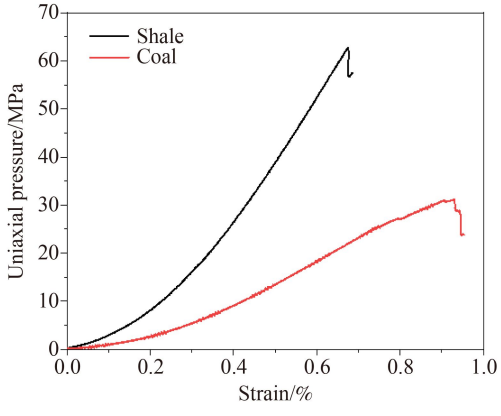

Fig. 7 Uniaxial compression curve of coal and shale.

Table 2 Difference of uniaxial compression parameters of coal and shale

Item	UCS/MPa	*E*/MPa	*U*/J
Coal	31.15	4512	25.72
Shale	62.72	12849	32.77

This difference in macroscopic properties of shale and coal is closely related to the internal pore structure of the two materials. According to the results of NMR experiments, the total porosity of coal is much higher than that of shale while the proportion of meso-macropores in coal is much higher than that of shale, which leads to more obvious pore defects in coal. Such a huge difference between micropore structures of coal and shale results in a significant expansion of micro-fractures during coal compression, which significantly affects the mechanical parameters.

3.3 Differences in Brazilian splitting characteristics

To compare the tensile failure characteristics in coal and shale, the Brazilian splitting test results of the two materials are shown in Fig. 8. Based on the force-displacement curves, the Brazilian splitting parameters were calculated and the obtained results are listed in Table 3. It is observed that the Brazilian splitting curves of coal and shale are similar to the uniaxial compression curve and consist of four stages. It is found that the plastic stage of shale is very short and has brittle characteristics, while coal has a significant plastic stage. According to the experimental results in Table 3, the average tensile strength and Brazilian splitting modulus of shale are 7.92 times and 6.68 times of coal, respectively, indicating that shale has a stronger tensile. Generally, the lower the E_B value of the rock, the weaker its brittleness and resistance to crack propagation, the more severe the damage to the internal structure, and weaken the elastic deformation resistance (Aybar et al., 2014; Gholami et al., 2016). Moreover, the U_B of shale is 10.78 times that of coal, indicating that the resistance of coal to damage is relatively weak, and coal is damaged by absorbing less energy. The *BI* value of shale is 4.37 times that of coal, indicating that coal has lower brittleness and higher ductility.

3.4 Difference in CO_2 adsorption capacity

The CO_2 adsorption of coal and shale under different particle sizes is shown in Fig. 9. It is observed that as the equilibrium pressure increases, the CO_2 adsorption capacity of coal and shale increases. At a constant equilibrium pressure, the CO_2 adsorption capacity increases with a decrease in particle size. The fitting

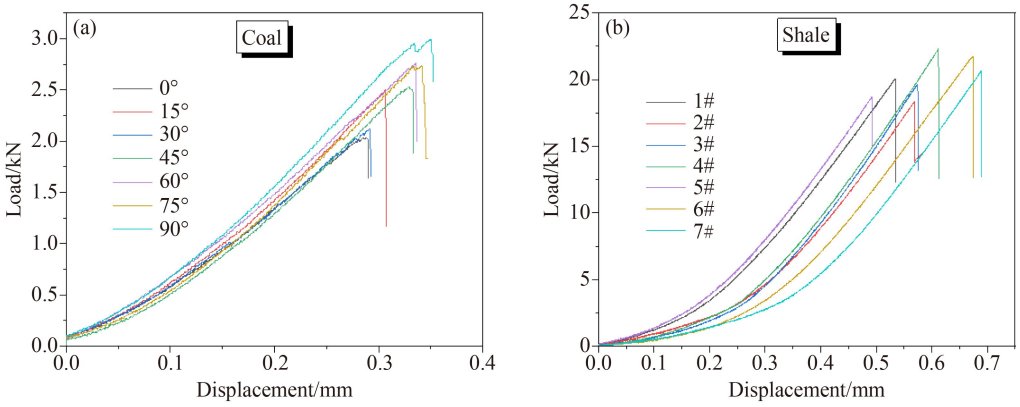

Fig. 8 Brazil splitting curve of coal and shale.

results of the Langmuir constant for coal and shale adsorption data are shown in Table 4. It is found that *a* values of coal and shale for a particle size < 0.074 mm are 1.54 and 1.88 times that of 1–3 mm, respectively. In addition, under the same equilibrium pressure and particle size, the adsorption capacity of coal for CO_2 is greater than that of shale, indicating that coal has a higher adsorption capacity than shale. This conclusion can also be obtained from the average *a* value of coal, which is 6.62 times that of shale.

4 Conclusions

In the present study, the porosity, mechanical parameters, and gas adsorption of coal and shale are compared. Based on the performed analyses and obtained results, the main achievements can be summarized as follows.

1) The total porosity of coal is 7.51 times that of shale, and shale is dominated by adsorption pores, while coal's adsorption pores and seepage pores are equally important. The micropores and minipores ratios in shale are 2.31

Table 3 Differences of Brazil splitting parameters between coal and shale

Item	Coal					Shale				
	P_{max}/kN	σ_t/MPa	E_B/MPa	U_B/mJ	*BI*	P_{max}/kN	σ_t/MPa	E_B/MPa	U_B/mJ	*BI*
1#	2.06	1.05	306	279	3.62	20.08	10.23	2175	3992	19.16
2#	2.53	1.29	322	342	4.19	18.35	9.35	1956	3733	16.43
3#	2.15	1.09	304	288	3.72	19.67	10.02	2108	3641	17.46
4#	2.55	1.30	310	371	3.90	22.3	11.36	2109	4575	18.59
5#	2.78	1.42	325	432	4.21	18.68	9.51	2252	3418	19.33
6#	2.77	1.41	334	428	4.06	21.77	11.09	2248	4750	16.45
7#	3.01	1.53	351	502	4.35	20.67	10.53	2210	4337	15.28
Average value	2.55	1.30	322	377	4.01	20.22	10.30	2151	4064	17.53

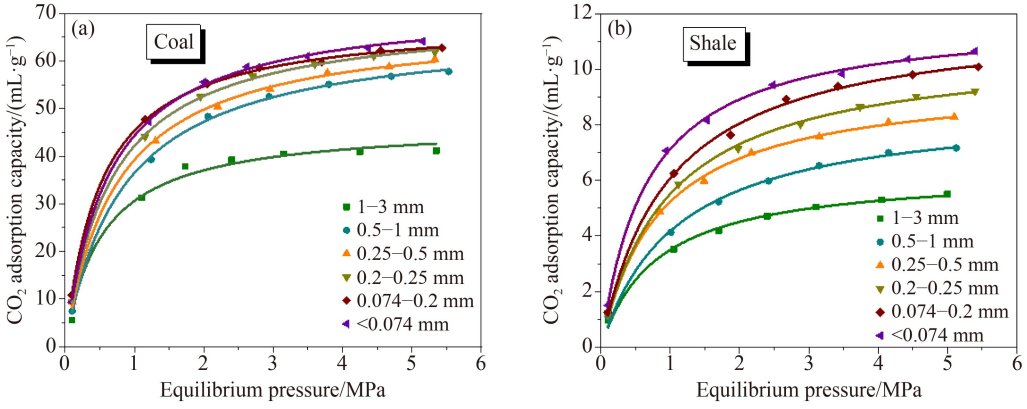

Fig. 9 CO_2 adsorption isotherms of coal and shale.

Table 4 Langmuir parameters of CO_2 adsorption isotherms of coal and shale

Item	Coal		Shale	
	a/(mL·g^{-1})	b/(MPa^{-1})	a/(mL·g^{-1})	b/(MPa^{-1})
1−3 mm	46.88	1.88	6.33	1.23
0.5−1 mm	67.01	1.19	8.73	0.92
0.25−0.5 mm	68.13	1.36	9.67	1.18
0.2−0.25 mm	70.09	1.51	10.83	1.04
0.074−0.2 mm	68.98	1.92	11.93	1.04
<0.074 mm	72.26	1.59	11.91	1.49
Average value	65.56	1.58	9.90	1.15

times and 1.08 times that of coal, respectively, while the mesopores and macropores of coal are 1.99 times and 31.39 times that of shale, respectively. The adsorption pore surface of coal is rougher than that of shale, and the seepage pore structure of shale is more complex.

2) Coal has significant stages, in which internal microcracks develop and propagate rapidly and obvious plastic deformations occur, while these two stages are very short in shale and it is obviously brittle. The UCS, E, and U of shale are 2.01 times, 2.85 times, and 1.27 times that of coal, respectively. It is concluded that shale has more compression resistance and resistance to elastic deformation than coal.

3) The average tensile strength and Brazilian splitting modulus of shale are 7.92 times and 6.68 times that of coal, respectively, indicating that shale has stronger tensile capacity. Meanwhile, the U_B of shale is 10.78 times that of coal, which indicates that coal has weak resistance to damage. In addition, the BI value of shale is 4.37 times that of coal, indicating that coal has lower brittleness and higher ductility.

4) The CO_2 adsorption capacities of coal and shale increase with the decrease in particle size. Under the same conditions, the CO_2 adsorption capacity of coal is greater than that of shale, and the average a value of coal is 6.62 times that of shale.

Acknowledgments This work was financially supported by the Jiangxi Provincial Thousand Talents Plan Project (No. jxsq2019102082).

References

Aybar U, Eshkalak M O, Sepehrnoori K, Patzek T W (2014). The effect of natural fracture's closure on long-term gas production from unconventional resources. J Nat Gas Sci Eng, 21: 1205–1213

Cao T T, Song Z G, Luo H Y, Liu G X (2015). The differences of microscopic pore structure characteristics of coal, oil shale and shales and their storage mechanisms. Nat Gas Geosci, 26(11): 2208–2218

Chandra D, Vishal V, Bahadur J, Sen D (2020). A novel approach to identify accessible and inaccessible pores in gas shales using combined low-pressure sorption and SAXS/SANS analysis. Int J Coal Geol, 228: 103556

Chen S, Zhu Y, Wang H, Liu H, Wei W, Luo Y, Li W, Fang J (2010). Research status and trends of shale gas in China. Acta Petrol Sin, 31(4): 689–694

Chen S, Tang D, Tao S, Ji X, Xu H. (2019). Fractal analysis of the dynamic variation in pore-fracture systems under the action of stress using a low-field NMR relaxation method: an experimental study of coals from western Guizhou in China. J Petrol Sci Eng, 173: 617–629

Feng G, Kang Y, Sun Z, Wang X, Hu Y (2019). Effects of supercritical CO_2 adsorption on the mechanical characteristics and failure mechanisms of shale. Energy, 173: 870–882

Gao S, Jia L, Zhou Q, Cheng H, Wang Y (2022). Microscopic pore structure changes in coal induced by a CO_2–H_2O reaction system. J Petrol Sci Eng, 208: 109361

Geng W, Huang G, Guo S, Jiang C, Dong Z, Wang W (2022). Influence of long-term CH_4 and CO_2 treatment on the pore structure and mechanical strength characteristics of Baijiao Coal. Energy, 242: 122986

Gholami R, Rasouli V, Sarmadivaleh M, Minaeian V, Fakhari N (2016). Brittleness of gas shale reservoirs: a case study from the north Perth Basin, Australia. J Nat Gas Sci Eng, 33: 1244–1259

Hou P, Xue Y, Gao F, Dou F, Su S, Cai C, Zhu C (2022). Effect of liquid nitrogen cooling on mechanical characteristics and fracture morphology of layer coal under Brazilian splitting test. Int J Rock Mech Min Sci, 151: 105026

Jin K, Cheng Y, Liu Q, Zhao W, Wang L, Wang F, Wu D (2016). Experimental investigation of pore structure damage in pulverized coal: implications for methane adsorption and diffusion characteristics. Energy Fuels, 30(12): 10383–10395

Joubert J I, Grein C T, Bienstock D (1973). Sorption of methane in moist coal. Fuel, 52(3): 181–185

Langmuir I (1918). The adsorption of gases on plane surfaces of glass, mica and platinum. J Am Chem Soc, 40(9): 1361–1403

Liu X, Zhang C, Nie B, Zhang C, Song D, Yang T, Ma Z (2022a). Mechanical response and mineral dissolution of anthracite induced by supercritical CO_2 saturation: influence of saturation time. Fuel, 319: 123759

Liu Z, Lin X, Cheng Y, Chen R, Zhao L, Wang L, Li W, Wang Z (2022b). Experimental investigation on the diffusion property of different form coal: implication for the selection of CO_2 storage reservoir. Fuel, 318: 123691

Liu Z, Lin X, Wang Z, Zhang Z, Chen R, Wang L, Li W (2022c). Modeling and experimental study on methane diffusivity in coal mass under in-situ high stress conditions: a better understanding of gas extraction. Fuel, 321: 124078

Satya, Harpalani, Basanta, K., Prusty, Pratik, et al. (2006). Methane/CO_2 sorption modeling for coalbed methane production and CO_2 sequestration. Energy Fuels, 20(4): 1591–1599

Shao X, Pang X, Li H, Zhang X (2017). Fractal analysis of pore network in tight gas sandstones using NMR Method: a case study from the Ordos Basin, China. Energy Fuels, 31(10): 10358–10368

Sing K (1982). Reporting physisorption data for gas/solid systems with special reference to the determination of surface area and porosity

(Provisional). Pure Appl Chem, 54(11): 2201–2218

Song Y, Zou Q, Su E, Zhang Y, Sun Y (2020). Changes in the microstructure of low-rank coal after supercritical CO_2 and water treatment. Fuel, 279: 118493

Su E, Liang Y, Chang X, Zou Q, Xu M, Sasmito AP (2020). Effects of cyclic saturation of supercritical CO_2 on the pore structures and mechanical properties of bituminous coal: an experimental study. J CO_2 Util, 40: 101208

Wang G, Qin X, Shen J, Zhang Z, Han D, Jiang C (2019). Quantitative analysis of microscopic structure and gas seepage characteristics of low-rank coal based on CT three-dimensional reconstruction of CT images and fractal theory. Fuel, 256: 115900

Wang H M, Zhu Y M, Li W, Zhang J S, Luo Y (2011). Two major geological control factors of occurrence characteristics of CBM. J China Coal Soc, 36(7): 1129–1134 (in Chinese)

Wang X, Cheng Y, Zhang D, Liu Z, Wang Z, Jiang Z (2021a). Influence of tectonic evolution on pore structure and fractal characteristics of coal by low pressure gas adsorption. J Nat Gas Sci Eng, 87: 103788

Wang X, Cheng Y, Zhang D, Yang H, Zhou X, Jiang Z (2021b). Experimental study on methane adsorption and time-dependent dynamic diffusion coefficient of intact and tectonic coals: implications for CO_2-enhanced coalbed methane projects. Process Saf Environ Prot, 156: 568–580

Wang X, Geng J, Zhang D, Xiao W, Chen Y, Zhang H (2022a). Influence of sub-supercritical CO_2 on pore structure and fractal characteristics of anthracite: an experimental study. Energy, 261: 125115

Wang X, Liu H, Zhang D, Yuan X, Zeng P, Zhang H (2022b). Effects of CO_2 adsorption on molecular structure characteristics of coal: implications for CO_2 geological sequestration. Fuel, 321: 124155

Wang X, Zhang D, Liu H, Jin Z, Yue T, Zhang H (2022c). Investigation on the influences of CO_2 adsorption on the mechanical properties of anthracite by Brazilian splitting test. Energy, 259: 125053

Wang X, Zhang D, Su E, Jiang Z, Wang C, Chu Y, Ye C (2020). Pore structure and diffusion characteristics of intact and tectonic coals: implications for selection of CO_2 geological sequestration site. J Nat Gas Sci Eng, 81: 103388

Wang Z, Fu X, Hao M, Li G, Pan J, Niu Q, Zhou H (2021c). Experimental insights into the adsorption-desorption of CH_4/N_2 and induced strain for medium-rank coals. J Petrol Sci Eng, 204: 108705

Wang Z, Pan J, Hou Q, Yu B, Li M, Niu Q (2018a). Anisotropic characteristics of low-rank coal fractures in the Fukang mining area, China. Fuel, 211: 182–193

Wang Z, Pan J, Hou Q, Niu Q, Tian J, Wang H, Fu X (2018b). Changes in the anisotropic permeability of low-rank coal under varying effective stress in Fukang mining area, China. Fuel, 234: 1481–1497

Wu T, Du X, Li Q (2020). Comparative analysis of pore structure and adsorption characteristics of coal and shale. Safe Coal Mines, 51(11): 6

Yang K, Zhou J, Xian X, Jiang Y, Zhang C, Lu Z, Yin H (2022a). Gas adsorption characteristics changes in shale after supercritical CO_2-water exposure at different pressures and temperatures. Fuel, 310: 122260

Yang K, Zhou J, Xian X, Zhou L, Zhang C, Tian S, Lu Z, Zhang F (2022b). Chemical-mechanical coupling effects on the permeability of shale subjected to supercritical CO_2-water exposure. Energy, 248: 123591

Yang Q, Li W, Jin K (2020). Supercritical CO_2 interaction induced pore morphology alterations of various ranked coals: a comparative analysis using corrected mercury intrusion porosimetry and low-pressure N_2 gas adsorption. ACS Omega, 5(16): 9276–9290

Yu Y, Wang T (2004). Study on relationship between splitting behaviour and elastic modulus of Three Gorges granite. Chinese J Rock Mechan Eng, 23(19): 3258–3261

Zhang K, Hou CH, Zhao DF, Guo YH, Hui XU (2017). Comparison of pore structure characteristics fractal characteristics between coal and shale through nitrogen adsorption experiment with the example of Shanxi Formation 15# Coal and shale in Yangquan Area. Sci Techn Eng, 29: 68–75

Zhang X G, Ranjith P G, Ranathunga A S, Li D Y (2019). Variation of mechanical properties of bituminous coal under CO_2 and H_2O saturation. J Nat Gas Sci Eng, 61: 158–168

Zheng J, Huang G, Cheng Q, Zhen L, Cai Y, Wang W (2022). Degradation of mechanical and microporous properties of coal subjected to long-term sorption. Fuel, 315: 123245

Zhou J, Xie S, Jiang Y, Xian X, Liu Q, Lu Z, Lyu Q (2018). Influence of supercritical CO_2 exposure on CH_4 and CO_2 adsorption behaviors of shale: implications for CO_2 sequestration. Energy Fuels, 32(5): 6073–6089